



Ground State of Quantum Spin Systems on the Triangular Lattice

Hidetoshi NISHIMORI and Hiizu NAKANISHI[†]*Department of Physics, Tokyo Institute of Technology,
Oh-okayama, Meguro-ku, Tokyo 152*[†]*Department of Physics, Faculty of Science and Technology,
Keio University, Hiyoshi, Kohoku-ku, Yokohama 223*

(Received September 12, 1987)

The ground states of quantum spin systems with spin $1/2$ are investigated on the triangular lattice by numerically diagonalizing finite size systems ($N \leq 27$). In the ferromagnetic and antiferromagnetic XY models the correlation functions are found to decay by power laws. The antiferromagnetic Heisenberg model is likely to be paramagnetic in the ground state. Thus the classical long-range order is destroyed by quantum effects in all of the models we studied.

§1. Introduction

While each spin points to definite direction in the ground state of a classical spin system, the situation is sometimes quite different in quantum spin systems due to quantum mechanical fluctuations around the classical ground state. One of the powerful tools to treat the quantum fluctuations is the spin wave theory.^{1,2)} This theory provides a method to estimate quantitatively the amount of quantum fluctuations by expanding physical quantities in powers of $1/s$ (s denotes the spin magnitude) and therefore enables us to determine whether or not the classical state concerned is stable against quantum mechanical perturbation. (Our argument here is limited to quantum effects at $T=0$ although thermal fluctuations are also treated by the spin wave theory.¹⁻³⁾) For example, the one-dimensional Heisenberg antiferromagnet with spin $1/2$ has no ground-state long-range order in contrast to the classical counterpart.⁴⁾ This fact is correctly anticipated by the spin wave theory from the infrared divergence (long-distance instability) which appears, for instance, in the expression of spin-spin correlation functions at $T=0$.⁵⁾

As for the two-dimensional quantum spin systems, the situation is somewhat conflicting. The spin wave approach yields finite quantum corrections to the classical ground state,^{1,2)}

which implies that a finite long-range order survives in the two-dimensional quantum spin systems. In spite of this, some recent investigations suggest that no long-range order exists in the ground state of two-dimensional quantum spin systems. First of all, Anderson⁶⁾ has proposed a resonating valence bond (RVB) state as an alternative to the classical structure in the ground state of the spin $1/2$ Heisenberg antiferromagnet on the triangular lattice. The RVB state is composed of pairs of singlet states distributed all over the lattice. The singlet pairs move around in the sense that many states with different spin pairings are superposed with essentially uniform weight in the RVB wave function. Apparently the RVB state does not have a long-range magnetic order and is presumably paramagnetic. To examine the amplitude of this RVB state in the ground state Oguchi *et al.*⁷⁾ have made a numerical analysis on finite size systems ($N \leq 21$). They found a relatively large projection of the finite system wave function onto the RVB state (although the projection decreases linearly with the system size). Their result also indicated only small value of the magnetic long-range order, if any, in the Heisenberg antiferromagnet on the triangular lattice. Possible breakdown of the spin wave prediction was further suggested by Fujiki and Betts (FB) in a series of numerical studies of finite size systems.⁸⁻¹¹⁾ They numerically

diagonalized ferromagnetic and antiferromagnetic XY models and antiferromagnetic Heisenberg model on the triangular lattice of sizes $N \leq 21$. By extrapolation to the infinite system ($N \rightarrow \infty$) they conjectured power decay of spin-spin correlation functions in all of those models. In other words the systems are critical at $T=0$.

If these predictions by three groups of authors are correct, the quantum spin systems on the triangular lattice are the first examples in which spin wave theory gives qualitatively incorrect results on the ground-state spin orderings. If this is the case, some non-perturbative (non-spin wave) mechanism would be playing a vital role in determining the ground-state properties of these quite quantum-mechanical systems. One should note here that one of the systems, the XY ferromagnet, has no frustration in the sense of Toulouse.¹²⁾ Therefore the possible non-perturbative mechanism referred to above does not have its origin in frustration at least in the XY ferromagnet. In these situations it should be quite important to determine whether the above-mentioned claims on the destruction of long-range order are reliable in the light of more extensive numerical data.

In the present paper we extend the work of Fujiki and Betts to larger systems ($N \leq 27$). Systematic extrapolation to the infinite system leads to the following conclusions: i) Both in the ferromagnetic and antiferromagnetic XY models the ground state is critical; both spin-spin and chirality (to be defined later for antiferromagnets) correlations would decay

algebraically. ii) The Heisenberg antiferromagnet is likely to be paramagnetic even in the ground state. These conclusions are consistent with breakdown of the spin wave picture, as suggested by previous authors, although details do not necessarily agree (*e.g.* Fujiki¹⁰⁾ suggests a power decay of the correlation function, instead of an exponential decay, in the Heisenberg case).

In the next section we describe the method and results of numerical investigation of the ferromagnetic XY model. The antiferromagnetic XY and Heisenberg models are treated subsequently. The last section is devoted to discussions.

§2. Ferromagnetic XY Model

2.1 Model and numerical method

For definiteness we write down here the Hamiltonian of our interest:

$$H = -\frac{J}{2} \sum_{\langle ij \rangle} (\sigma_i^x \sigma_j^x + \sigma_i^y \sigma_j^y + \Delta \sigma_i^z \sigma_j^z), \quad (2.1)$$

where σ_i denotes the Pauli spin operator. In the present section we concentrate on the XY ferromagnet ($J=1, \Delta=0$). The XY antiferromagnet ($J=-1, \Delta=0$) and Heisenberg antiferromagnet ($J=-1, \Delta=1$) will be discussed in §3 and §4. Following FB⁸⁾ we adopt equilateral parallelograms with $N(=3, 4, 7, \dots, 25, 27)$ lattice sites to cover the triangular lattice as depicted in Fig. 1. The boundaries are periodic in both directions.

To generate matrix elements of the Hamiltonian (2.1) we first have to determine the base states. Since the ground state of the present

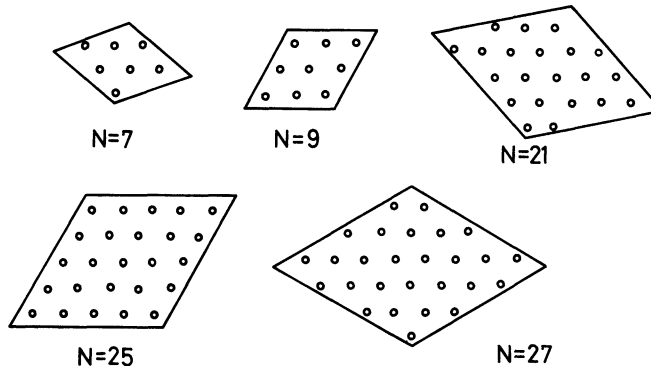


Fig. 1. Some of the lattices investigated in this paper. Boundary conditions are periodic in both directions.

system does not have a spontaneous magnetization along the z -axis, we are allowed to restrict ourselves to the subspace with minimum $M_z \equiv \sum \sigma_i^z/2$ (which is a good quantum number):¹³⁾ $M_z=0$ or $\pm 1/2$ depending upon whether N is even or odd. For $N \leq 21$ we were able to diagonalize the Hamiltonian in this subspace without using any additional symmetry. We inspected the resulting wave functions in view of the symmetry properties and found that a ground state is always invariant under translations and the operations of the point group C_{6v} . Hence, for larger lattices ($N=25$ and 27), we assumed the above mentioned symmetries in constructing the base states of matrix representation of the Hamiltonian since diagonalization without using space symmetry was impossible for these systems. The reduced spaces of states have dimensions 17,802 ($N=25$) and 63,202 ($N=27$). Systematic calculations were performed only on the largest two lattices ($N=25$ and 27) since full data for smaller systems are already available in FB's papers.⁸⁻¹¹⁾ The eigenvalues were calculated by the Lanczos method and the eigenvectors were obtained by the inverse iteration method supplemented by the conjugate gradient method.* The whole computation (including the XY and Heisenberg antiferromagnets) consumed about 15 hours of CPU time on the vector processor HITAC S-810/20 at the Computer Center of the University of Tokyo. Most of the time was devoted to the matrix construction and the diagonalization took only a small fraction.

We have found no degeneracy in the ground state of the XY ferromagnet, except the trivial Kramers degeneracy for odd N , as generally expected.¹³⁾

2.2 Short-range order

As has been observed by FB,⁸⁾ the ground-state energy per bond when plotted as a function of $1/N$ (Fig. 2, see also Table I in which data for $N \leq 21$ have been taken from FB's paper.⁸⁾ The same is true in all other Tables.) follows different trends depending on whether N is even or odd. The extrapolation to $N \rightarrow \infty$

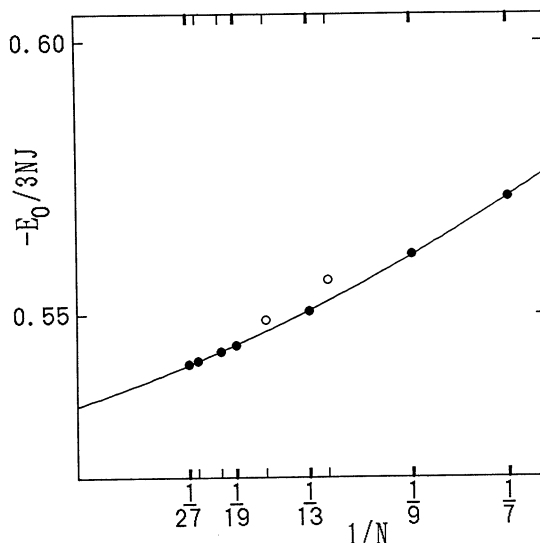


Fig. 2. The ground-state energy of the ferromagnetic XY model as a function of the inverse of the system size. The even- N data ($N=12$ and 16 as marked by white circles) follow different trends. The least-squares fit (solid line) extrapolates the finite- N values to the infinite-lattice estimate 0.5332.

Table I. Transverse correlation functions $\langle \sigma_0^x \sigma_n^x \rangle$ between n th neighboring spins for the ferromagnetic XY model at $T=0$. The data for $N \leq 21$ are taken from FB,⁸⁻¹¹⁾ which is the case in all the following Tables.

N	$n=1$	$n=2$	$n=3$	$n=4$	$n=5$
3	0.66667				
4	0.66667				
7	0.57143				
9	0.56103	0.52111			
12	0.55624	0.51188	0.50831		
13	0.55052	0.50295			
16	0.54891	0.49534	0.49531		
19	0.54423	0.48946	0.48422		
21	0.54309	0.48666	0.48182	0.47586	
25	0.54142	0.48317	0.47751	0.47034	
27	0.54079	0.48221	0.47550	0.46908	0.46674

is thus carried out by dropping the even- N ($=4, 12, 16$) data because there are more data for odd N ($=3, 7, 9, \dots, 25, 27$). A least-squares fit to a quadratic in $1/N$ yields the solid curve in Fig. 2, leading to

$$-E_0/3NJ = \langle \sigma_0^x \sigma_1^x \rangle = 0.5332 \pm 0.002, \quad (2.2)$$

in the limit $N \rightarrow \infty$. The uncertainty is estimated from scatterings in quadratic fits of data for various combinations of N 's. The

* The computer program was written as a slight modification of the diagonalization routine TITPACK which is for non-symmetry-reduced matrix.¹⁴⁾

Table II. Longitudinal correlation functions $\langle \sigma_0^z \sigma_n^z \rangle$ for the ferromagnetic XY model.

N	$n=1$	$n=2$	$n=3$	$n=4$	$n=5$
3	-0.33333				
4	-0.33333				
7	-0.14286				
9	-0.13408	-0.04221			
12	-0.13434	-0.03948	-0.03775		
13	-0.12446	-0.02939			
16	-0.12549	-0.02748	-0.02740		
19	-0.11853	-0.02093	-0.01843		
21	-0.11749	-0.01940	-0.01708	-0.01429	
25	-0.11596	-0.01750	-0.01487	-0.01167	
27	-0.11516	-0.01691	-0.01402	-0.01104	-0.01011

result (2.2) is in good agreement with FB's 0.5326 ± 0.003 obtained from smaller-lattice data. Other short-range orders (Tables I and II) are analyzed in a similar way to yield

$$\langle \sigma_0^z \sigma_1^z \rangle = -0.107 \pm 0.001, \quad (2.3)$$

$$\langle \sigma_0^z \sigma_2^z \rangle = 0.463 \pm 0.02, \quad (2.4)$$

$$\langle \sigma_0^z \sigma_2^z \rangle = -0.008 \pm 0.006. \quad (2.5)$$

The first one (2.3) represents the nearest neighbor zz -correlation whereas the rest are the next nearest neighbor correlations. The extrapolation of the latter is based on the data for $9 \leq N \leq 27$ since the $N=7$ lattice does not accommodate next nearest neighbors (Fig. 1). The four-spin correlation functions on the neighboring four sites (Fig. 3) have also been evaluated (Table III). By least-squares fits to quadratics in $1/N$ we obtain

$$\langle \sigma_1^x \sigma_2^x \sigma_3^x \sigma_4^x \rangle = 0.421 \pm 0.002, \quad (2.6)$$

$$\langle \sigma_1^x \sigma_2^x \sigma_3^y \sigma_4^y \rangle = 0.170 \pm 0.007, \quad (2.7)$$

$$\langle \sigma_1^x \sigma_2^y \sigma_3^y \sigma_4^x \rangle = 0.088 \pm 0.03. \quad (2.8)$$

All these estimates agree impressively with those of FB.⁸⁾ This fact confirms reliability of the present extrapolations.

2.3 Long-range order

A standard measure of magnetic long-range order in quantum systems is the square of the total magnetization:

$$M^2 = \left\langle \left(\sum_j \sigma_j \right)^2 \right\rangle / 4. \quad (2.9)$$

The brackets denote the expectation value with respect to the ground-state wave func-

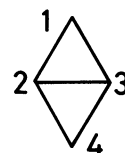


Fig. 3. Relation of four sites for which the four-spin correlations are calculated.

Table III. Four-spin correlation functions in the ferromagnetic XY model.

N	$\langle \sigma_1^x \sigma_2^x \sigma_3^x \sigma_4^x \rangle$	$\langle \sigma_1^x \sigma_2^y \sigma_3^y \sigma_4^x \rangle$	$\langle \sigma_1^x \sigma_2^x \sigma_3^y \sigma_4^y \rangle$
9	0.47873	0.13100	0.17369
12	0.47051	0.12498	0.17277
13	0.45715	0.11796	0.16960
16	0.45359	0.11183	0.17088
19	0.44365	0.10771	0.16797
21	0.44117	0.10560	0.16779
25	0.43767	0.10299	0.16725
27	0.43620	0.10282	0.16713

tion. Since the magnetization in the z -direction $\sum_j \sigma_j^z / 2$ is either $\pm 1/2$ (N odd) or 0 (N even), eq. (2.9) effectively measures spin ordering in the XY plane. By investigating M^2 as a function of N we can find out whether the ground state is ordered or not: Finiteness of long-range spin-spin correlation leads to a quadratic dependence of eq. (2.9) on the system size N because of the double sum. If, on the other hand, the correlation function decays algebraically (power law) as

$$\langle \sigma_0^x \sigma_r^x \rangle \sim r^{-\eta}, \quad (2.10)$$

then M^2 in eq. (2.9) is expected to depend on N as $N^{2-\eta/2}$ in the leading order as can be verified by integrating eq. (2.10). The third possibility is an exponential decay of correlation function (i.e. paramagnetic ground state), which will be reflected in N -linear behavior of the expectation value (2.9) (or $\eta=2$ if fitted to $N^{2-\eta/2}$).

Following FB⁸⁾ we fit the quantity $4M^2/N^2 - 2/N$ (listed in Table IV) to two functional forms

$$f_1(1/N) = A_1 + B_1/N + C_1/N^2, \quad (2.11)$$

$$f_2(1/N) = N^{-\eta/2}(A_2 + B_2/N). \quad (2.12)$$

Subtraction of $2/N$ in the definition above stems from corrections of autocorrelation effects: In the Heisenberg ferromagnet with spin $1/2$, the order parameter $4M^2$, eq. (2.9),

Table IV. Long-range order in the ferromagnetic XY model and the residuals (fitting errors) resulting from the fitting functions (2.13) and (2.14).

N	$4M^2/N^2 - 2/N$ ($\equiv f$)	$(f-f_1) \times 10^5$	$(f-f_2) \times 10^5$
7	1.0000	81	3
9	0.9920	-186	-19
12	0.9816	-13	23
13	0.9784	38	23
16	0.9689	81	-27
19	0.9615	115	2
21	0.9567	66	-12
25	0.9484	-65	-13
27	0.9450	-116	22

has the value $N^2 + 2N$ in the ground state, the second term $2N$ merely representing autocorrelation irrelevant to long-range order. For this reason FB⁸⁾ suggest $4M^2/N^2 - 2/N$ instead of $4M^2/N^2$ as the measure of long-range order. The first function f_1 implies a finite long-range order A_1 in the limit $N \rightarrow \infty$ whereas f_2 comes from the power-decaying correlation (2.10). The best fits to data for $7 \leq N \leq 27$ were obtained by

$$f_1 = 0.90383 + 1.30960/N - 4.49411/N^2, \quad (2.13)$$

$$f_2 = N^{-0.11906/2} (1.15896 - 0.25321/N), \quad (2.14)$$

which are shown in Fig. 4. Although the second fitting function (2.14) may at first seem somewhat bold (see the full line in the inset of Fig. 4), we prefer this to eq. (2.13) for the following reasons: (i) Residuals (differences between the data and the values predicted by a fitting function) are much smaller in f_2 than in f_1 (see Table IV). (ii) The fitting parameters η , A_2 and B_2 have much less dependence on N as compared to A_1 , B_1 and C_1 . In fact FB⁸⁾ tried the same fitting functions (2.11) and (2.12) for smaller lattices ($N \leq 21$) and their results are

$$f_1^{\text{FB}} = 0.91090 + 1.14929/N - 3.69587/N^2,^* \quad (2.15)$$

$$f_2^{\text{FB}} = N^{-0.12060/2} (1.16222 - 0.26426/N). \quad (2.16)$$

By comparing eqs. (2.15) and (2.16) with (2.13) and (2.14) we see more stability in the

* The sign of the last term in this equation is written as + in FB's paper,⁸⁾ which is simply a typographic error.

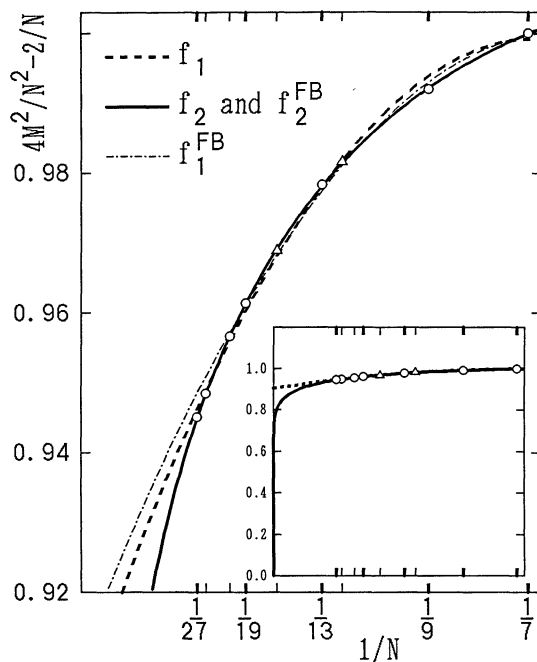


Fig. 4. The order parameter $4M^2/N^2 - 2/N$ of the ferromagnetic XY model. The fitting functions f_1 (2.13), f_2 (2.14), f_1^{FB} (2.15), and f_2^{FB} (2.16) are shown by curves. Two curves f_2 and f_2^{FB} cannot be distinguished in this scale. In the inset the fitting functions f_1 and f_2 are given by a full scale.

coefficients of f_2 than in those of f_1 . We conclude that the function f_2 is more likely to explain the asymptotic $N \rightarrow \infty$ behavior than f_1 . Consequently the spin-spin correlation function in the XY plane decays algebraically (2.10) with the exponent $\eta \sim 0.12$. No long-range order is sustained by the present quantum spin system. Let us note that this conclusion is the same one as FB's,⁸⁾ including the exponent value $\eta \sim 0.12$. Our new contribution here is that we discriminated f_2 from f_1 more convincingly than FB did because their data for $N \leq 21$ gave much less difference between these two fitting functions.

§3. Antiferromagnetic XY Model

3.1 Symmetry of the ground state

In the ground state of the classical antiferromagnetic XY model the lattice is divided into three sublattices each of which has a definite spin direction (Fig. 5). The relative orientation between spins on different sublattices is $\pm 2\pi/3$. It is therefore natural in the in-



Fig. 5. Two degenerate ground-state structures of the classical XY and Heisenberg antiferromagnets. The symbols + and - denote the chirality degree of freedom.

vestigation of quantum systems to exclude the systems with the number of sites not multiple of three. We are left with $N=3, 9, 12, 21, 27$. The reduction of matrix size described in §2.1 needs modification because of the three-sublattice structure. While in the ferromagnetic case the full translational and rotational (C_{6v}) invariance was employed, the ground states of antiferromagnet are invariant under the operations which leave the sublattices invariant as we checked the non-symmetry-reduced eigenstates for $N \leq 21$. Accordingly FB⁹⁾ used base states with sublattice-translation invariance and C_3 rotation invariance. The latter corresponds to the rotation within the same sublattice, see Fig. 5. We adopt here, however, C_{6v} symmetry instead of C_3 on the basis of the following properties confirmed in the $N \leq 21$ systems. The ground state has a four-fold degeneracy, two in the space $M_z=1/2$ and the other two in $M_z=-1/2$. In each of these spaces one of the ground states can be chosen to be “ C_6 -symmetric” and the other “ C_6 -antisymmetric”, namely, the one is invariant under all the C_{6v} operations (irreducible representation A_1) and the other changes sign under the $2\pi/6$ rotation (irreducible representation B_1).¹⁵⁾ This degeneracy of C_6 -symmetric and antisymmetric states would correspond to two possible linear combinations of the degenerate classical states in Fig. 5. The first combination with the same sign of Figs. 5(a) and 5(b) is C_6 -symmetric and the second with an opposite sign is C_6 -antisymmetric. Therefore it suffices to consider the C_6 -symmetric state as a representative wave function for the investigation of spin ordering. The reduced matrix is of dimensions 188,724 for $N=27$. After completion of the matrix construction, diagonalization proceeded just as in the ferromagnetic case.

3.2 Short-range order

The data of short-range correlation functions are given in Tables V, VI and VII. Extrapolation to the infinite size $N \rightarrow \infty$ was performed by using the data of $N=9, 21, 27$. The even-site lattice $N=12$ apparently falls on a different series in its N -dependence and was dropped off from analysis.

The transverse correlations $\langle \sigma_0^x \sigma_1^x \rangle$ and $\langle \sigma_0^x \sigma_2^x \rangle$, where 0 and 1 are the nearest neighbors and 0 and 2 are the next nearest neighbors, and the four-spin correlations behave in a fairly regular manner as functions of $1/N$ (see Figs. 6–8). For each correlation the coefficients of the quadratic fitting function $f(1/N)=a+b/N+c/N^2$ were determined such that the data values at $N=9, 21$, and 27 were reproduced correctly. The first coefficient a gives the limiting estimate as $N \rightarrow \infty$. The results are

Table V. Transverse correlation functions $\langle \sigma_0^x \sigma_n^x \rangle$ in the antiferromagnetic XY model.

N	$n=1$	$n=2$	$n=3$	$n=4$	$n=5$
3	-0.33333				
9	-0.28274	0.48966			
12	-0.28612	0.38780	-0.15695*		
21	-0.27524	0.44281	-0.21556	-0.21960	
27	-0.27446	0.43329	-0.20669	-0.21165	0.41282

* In FB’s Table I, ref. 9, this number is written as -0.19695, which is a typographic error.

Table VI. Longitudinal correlation functions $\langle \sigma_0^z \sigma_n^z \rangle$ in the antiferromagnetic XY model.

N	$n=1$	$n=2$	$n=3$	$n=4$	$n=5$
3	-0.33333				
9	-0.15504	0.02069			
12	-0.19510	0.08064	-0.03564		
21	-0.14108	0.00557	-0.01789	-0.01600	
27	-0.14083	0.00781	-0.01373	-0.01194	-0.00544

Table VII. Four-spin correlation functions in the antiferromagnetic XY model.

N	$\langle \sigma_1^x \sigma_2^x \sigma_3^x \sigma_4^x \rangle$	$\langle \sigma_1^x \sigma_2^y \sigma_3^y \sigma_4^x \rangle$	$\langle \sigma_1^x \sigma_2^x \sigma_3^y \sigma_4^y \rangle$
9	0.05126	-0.30789	0.17958
12	0.14590	-0.24210	0.19400
21	0.07682	-0.27065	0.17374
27	0.08269	-0.26404	0.17336

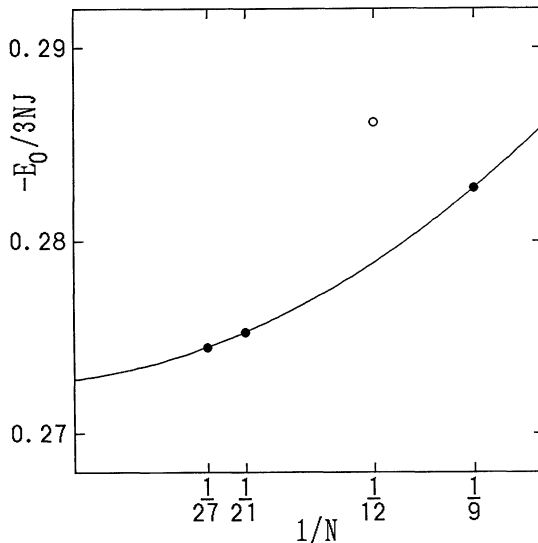


Fig. 6. Ground-state energy of the antiferromagnetic XY model. The solid curve represents quadratic extrapolations of $N=9, 21, 27$ data.

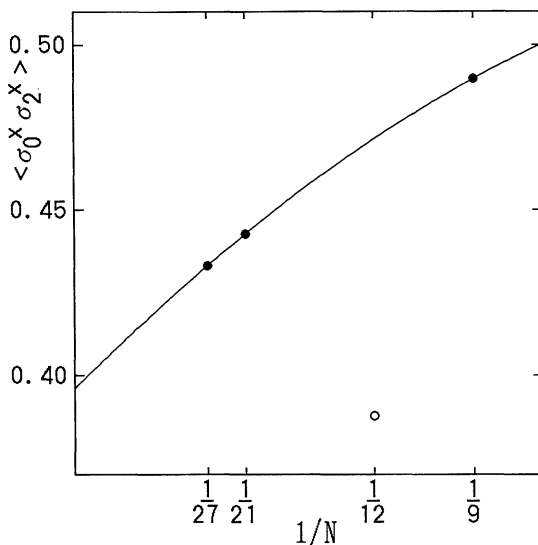


Fig. 7. Next nearest neighbor transverse correlation of the antiferromagnetic XY model. Extrapolation is carried out by the quadratic curve.

$$\langle \sigma_0^x \sigma_1^x \rangle = E_0/3N|J| = -0.2728 \pm 0.002, \quad (3.1)$$

$$\langle \sigma_0^x \sigma_2^x \rangle = 0.3961 \pm 0.024, \quad (3.2)$$

$$\langle \sigma_1^x \sigma_2^x \sigma_3^y \sigma_4^y \rangle = 0.1734 \pm 0.009, \quad (3.3)$$

$$\langle \sigma_1^x \sigma_2^y \sigma_3^y \sigma_4^x \rangle = -0.2400 \pm 0.006, \quad (3.4)$$

$$\langle \sigma_1^x \sigma_2^x \sigma_3^x \sigma_4^x \rangle = 0.1069 \pm 0.014. \quad (3.5)$$

The uncertainties represent twice of the difference between our estimates (from $N=9,$

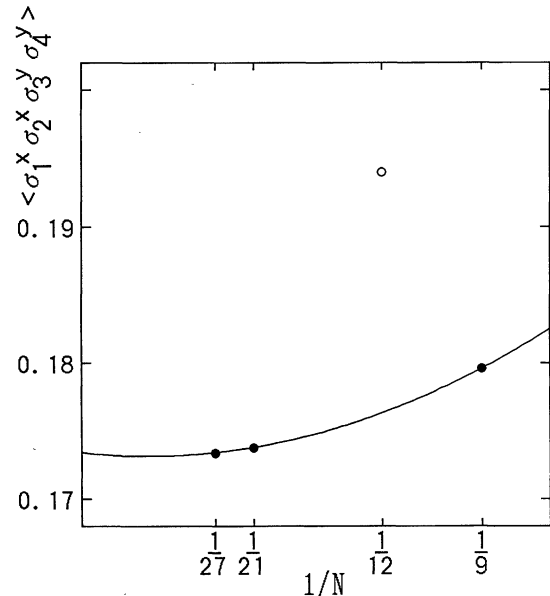


Fig. 8. Four-spin correlation function in the ground state of the antiferromagnetic XY model. Quadratic curve extrapolates finite-size data to $N \rightarrow \infty$.

21, 27) and those of FB (from $N=3, 9, 21$). This determination of confidence limits is rather arbitrary. Nevertheless smallness of the resulting error bars as written in the above equations confirms reliability of the estimates.

The zz -correlation functions show somewhat erratic behavior (Figs. 9 and 10). As to the nearest neighbor correlation $\langle \sigma_0^z \sigma_1^z \rangle$ we tried both quadratic and linear fitting functions (the latter by least-squares) as

$$\langle \sigma_0^z \sigma_1^z \rangle = -0.14463 + 0.20066/N - 2.64931/N^2, \quad (3.6)$$

$$\langle \sigma_0^z \sigma_1^z \rangle = -0.13249 - 0.20161/N. \quad (3.7)$$

We accepted -0.1386 (average of $c_1 \equiv -0.14463$ and $c_2 \equiv -0.13249$) with uncertainty of ± 0.012 (difference of c_1 and c_2). The next nearest neighbor correlation $\langle \sigma_0^z \sigma_2^z \rangle$ was analyzed by a least-squares method (Fig. 10) leading to

$$\langle \sigma_0^z \sigma_2^z \rangle = -0.0015 \pm 0.009. \quad (3.8)$$

The uncertainty corresponds to twice of the difference between our estimate and FB's.⁹⁾

In the classical antiferromagnetic XY model each plaquette has an Ising-like variable called chirality.¹⁶⁾ This quantity denotes the sense of rotation of spin angle as one goes round the

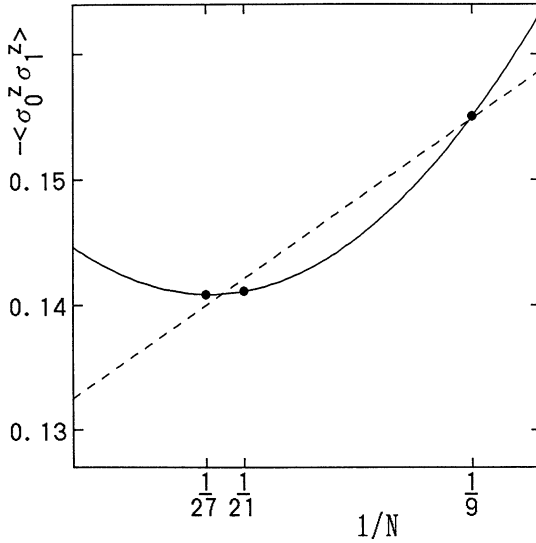


Fig. 9. The nearest neighbor longitudinal correlation of the antiferromagnetic XY model. The solid curve denotes a quadratic fit while the broken line is a least-squares fit to a linear function.

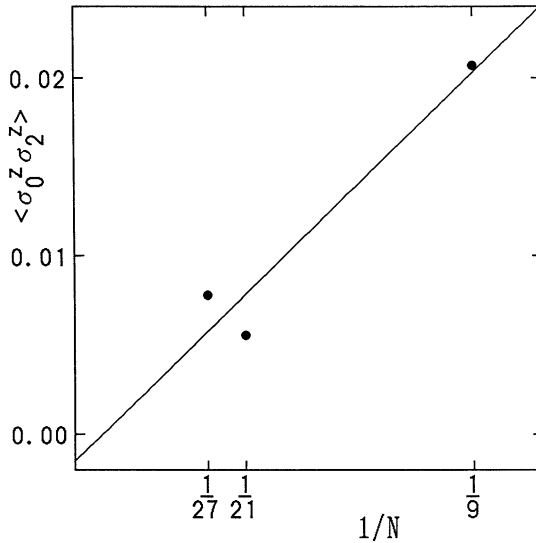


Fig. 10. The next nearest neighbor longitudinal correlation of the antiferromagnetic XY model. Extrapolation to $N \rightarrow \infty$ is carried out by a least-squares fit to a linear function.

plaquette (see Fig. 5). Chirality is known to attach an Ising character to the thermodynamic phase transition of the classical system.¹⁷⁾ For this reason FB stressed the special significance of the quantum version of the chirality variable

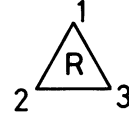


Fig. 11. We associate chirality $X(R)$, eq. (3.9), to a triangular plaquette.

$$X(R) \equiv (\sigma_1 \times \sigma_2 + \sigma_2 \times \sigma_3 + \sigma_3 \times \sigma_1) / 2\sqrt{3}, \quad (3.9)$$

where R denotes the plaquette determined by three sites 1, 2, and 3 (Fig. 11). A component, say X_z , has eigenvalues $-1, 0, 1$. Simple calculations show

$$\begin{aligned} -\langle X_z(R)X_z(R') \rangle &= (1 - 4\langle \sigma_1^x \sigma_2^x \rangle - \langle \sigma_1^z \sigma_2^z \rangle + 2\langle \sigma_1^x \sigma_4^x \rangle \\ &\quad - 2\langle \sigma_1^x \sigma_2^y \sigma_3^y \sigma_4^x \rangle + 2\langle \sigma_1^x \sigma_3^y \sigma_3^y \sigma_4^y \rangle) / 6 \\ &= 0.641 \pm 0.02, \end{aligned} \quad (3.10)$$

where sites are numbered as in Fig. 3. The extrapolated values in eqs. (3.1) to (3.7) were used in the last line. Fujiki¹⁰⁾ quotes 0.645 ± 0.02 as his estimate, a close value to ours.

3.3 Long-range order of twisted magnetization

The classical ground state has a rigid $2\pi/3$ structure, Fig. 5. The parameter to represent long-range order in the quantum system should take this fact into account. FB⁹⁾ thus proposed to calculate the expectation value of the square of the twisted magnetization

$$N_I \equiv \left(\sum_{j \in A} \sigma_j^x + \sum_{j \in B} \sigma_j^u + \sum_{j \in C} \sigma_j^v \right) / 2, \quad (3.11)$$

where A, B, C denote three sublattices. The operators σ_j^u and σ_j^v are defined as

$$\sigma_j^u = -\sigma_j^x / 2 + \sqrt{3} \sigma_j^y / 2, \quad (3.12)$$

$$\sigma_j^v = -\sigma_j^x / 2 - \sqrt{3} \sigma_j^y / 2, \quad (3.13)$$

so that the quantization axes are rotated by $\pm 2\pi/3$. The expectation value $\langle N_I^2 \rangle$ can be calculated from the data in Table V. The analysis proceeds quite analogously as in the XY ferromagnet. Following FB⁹⁾ we concentrate on

$$n^2 \equiv 8\langle N_I^2 \rangle / N^2 - 1/N, \quad (3.14)$$

so that autocorrelations do not affect our

analysis significantly.* We adjusted the coefficients of the fitting functions (2.11) and (2.12) to reproduce the data for n^2 of sizes $N=9, 21, 27$ to find

$$f_1 = 0.3673 + 2.4610/N - 10.0040/N^2 \quad (3.15)$$

$$f_2 = N^{-0.1699}(0.7921 - 0.3676/N). \quad (3.16)$$

We accept the second fitting function (3.16) for a power decay rather than the first one (3.15) which implies a finite long-range order. The reasons are (i) that the leading order constant 0.3673 in eq. (3.15) is fairly smaller than the corresponding 0.4073 obtained by FB⁹⁾ from data of $N=3, 9, 21$ and (ii) that the coefficients in eq. (3.15) steadily increase as the power of $1/N$ rises, which suggests inappropriateness of this expansion. In contrast to (i) above, the coefficients in the power-law fitting function (3.16) change very little from those of FB⁹⁾ ($N=3, 9, 21$):

$$f_2^{\text{FB}} = N^{-0.1699}(0.7922 - 0.3678/N). \quad (3.17)$$

Therefore we conclude that the power-law fitting function (3.16) correctly describes the asymptotic behavior as $N \rightarrow \infty$. This readily implies

$$\langle \sigma_i^x \sigma_r^x \rangle \sim r^{-\eta} \quad (\eta = 0.1699 \times 2 = 0.34), \quad (3.18)$$

where 0 and r are located on the same sublattice. In the present XY antiferromagnet quantum fluctuations destroy the classical long-range order in a more drastic manner as compared to the ferromagnetic case which has $\eta = 0.12$.

3.4 Long-range order of chirality

As mentioned in §3.2 the classical antiferromagnetic XY model on the triangular lattice possesses a discrete degree of freedom, chirality. In the ground state of the classical system of rigid spin structure this chirality has a long-range correlation. Since quantum fluctuations may destroy the chirality long-range order, as well as the conventional (twisted) magnetic order, FB¹¹⁾ analyzed the expectation value of the square of

$$\chi \equiv \sum_{R \in \mathcal{A}} X_z(R). \quad (3.19)$$

* The right hand side of FB's⁹⁾ eq. (4.8) has a typographic error and should be read $8\langle N_i^2 \rangle / N^2 - 1/N$.

Table VIII. Chirality long-range order $\langle \chi^2 \rangle / N^2$ for the antiferromagnetic XY and Heisenberg models.

N	XY	Heisenberg
3	1.00000	1.00000
9	0.69462	0.49383
12	0.58122	0.38926
21	0.61427	0.27391
27	0.59674	0.21257

Here the sum is over all upright triangles (denoted + in Fig. 5(a)) and the operator on the right hand side is the z -component of chirality (3.9). The data for $N=9, 21, 27$ given in Table VIII are put in the trial forms as before:

$$\langle \chi^2 \rangle / N^2 = 0.5261 + 2.1032/N - 5.2775/N^2, \quad (3.20)$$

$$\langle \chi^2 \rangle / N^2 = N^{-0.07353}(0.7324 + 0.7564/N). \quad (3.21)$$

In this case of chirality order parameter it is more difficult to choose one of the two fitting functions (3.20) and (3.21) than in the magnetic long-range order because the similar fitting functions by FB¹¹⁾ ($N=3, 9, 21$) include the pure autocorrelation data $N=3$ and are thus rather unreliable. That is, we are unable to check relative stability of coefficients in eqs. (3.20) and (3.21) as N increases. Nevertheless we observe steadily increasing coefficient in eq. (3.20) whereas the two coefficients 0.7324 and 0.7564 in eq. (3.21) are of the same order. This is the reason we tentatively conclude here that a power decay of chirality correlation with the exponent $\bar{\eta} = 0.15 (= 0.0735 \times 2)$ is more plausible than a finite chirality long-range order. Let us stress once again that the prediction of FB¹¹⁾ (a finite long-range order) should be taken with special caution because their analysis strongly depends upon the value of the pure autocorrelation term ($N=3$).

Thus we arrive at the picture that both magnetic and chirality long-range orders decay by power laws. This observation indicates breakdown of the classical state in a non-perturbative way as discussed in the Introduction. Finite temperature properties may be changed in a pronounced way from the classical counterpart. Further discussions are

given in §5.

§4. Antiferromagnetic Heisenberg Model

4.1 Short-range order

Symmetry of the ground state of the antiferromagnetic quantum Heisenberg model is the same as that of the antiferromagnetic XY model. The same base states as described in §3.1 were used to construct the matrix elements. Numerical data on correlation functions are given in Tables IX and X. As seen in Fig. 12 the $1/N$ dependence of short-range correlations is not quite systematic. If a quadratic fit were adopted for $\langle\sigma_0^x\sigma_1^x\rangle$ (Fig. 12), the difference between $N=9$ and 21 would be overstressed as a large curvature, leading to non-monotonic behavior (upturn near $1/N\sim 0$). We thus use a least-squares fit to a linear form $a+b/N$ using data of $N=9, 21, 27$. The extrapolated values of this and other correlation functions are

$$\langle\sigma_0^x\sigma_1^x\rangle=2E_0/9N|J|=-0.2431\pm 0.004, \quad (4.1)$$

$$\langle\sigma_0^x\sigma_2^x\rangle=0.1605\pm 0.007, \quad (4.2)$$

$$\langle\sigma_1^x\sigma_2^x\sigma_3^x\sigma_4^x\rangle=0.1896\pm 0.009, \quad (4.3)$$

$$\langle\sigma_1^x\sigma_2^y\sigma_3^y\sigma_4^x\rangle=-0.0993\pm 0.002, \quad (4.4)$$

$$\langle\sigma_1^x\sigma_2^x\sigma_3^y\sigma_4^y\rangle=0.1377\pm 0.01. \quad (4.5)$$

The uncertainties represent difference of our limiting values as $N\rightarrow\infty$ and those of Fujiki.¹⁰ The chirality short-range order is found to be

$$\langle X_z(R)X_z(R')\rangle=-0.502\pm 0.02, \quad (4.6)$$

Table IX. Correlation functions $\langle\sigma_0^x\sigma_n^x\rangle$ for the antiferromagnetic Heisenberg model.

N	$n=1$	$n=2$	$n=3$	$n=4$	$n=5$
3	-0.33333				
9	-0.25926	0.33333			
12	-0.27126	0.25735	-0.07225		
21	-0.24933	0.23666	-0.10222	-0.13152	
27	-0.24899	0.21656	-0.07379	-0.11000	0.16717

Table X. Four-spin correlation functions for the antiferromagnetic Heisenberg model.

N	$\langle\sigma_1^x\sigma_2^x\sigma_3^x\sigma_4^x\rangle$	$\langle\sigma_1^x\sigma_2^y\sigma_3^y\sigma_4^x\rangle$	$\langle\sigma_1^x\sigma_2^x\sigma_3^y\sigma_4^y\rangle$
9	0.10124	-0.18025	0.14074
12	0.19783	-0.15931	0.17857
21	0.14930	-0.13448	0.14188
27	0.16205	-0.12596	0.13647

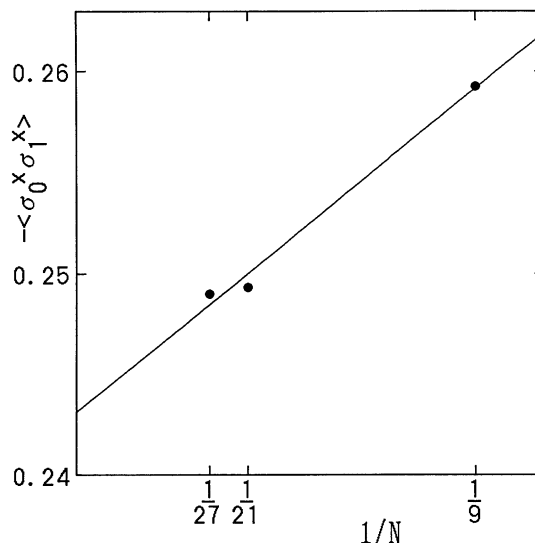


Fig. 12. The nearest neighbor correlation $\langle\sigma_0^x\sigma_1^x\rangle$ of the antiferromagnetic Heisenberg model. The line indicates extrapolation to $N\rightarrow\infty$ by least squares.

which is to be compared with -0.507 ± 0.02 of Fujiki.¹⁰

4.2 Long-range order of twisted magnetization

As in the antiferromagnetic XY model we have two types of long-range orders to be investigated, the twisted magnetic order and the chirality order. First, the twisted magnetization (3.11) is analyzed by using the combination

$$n^2\equiv 12\langle N_l^2\rangle/N^2-2/N, \quad (4.7)$$

following Fujiki.¹⁰ Again the two fitting functions (2.11) and (2.12) to the data for $N=9, 21, 27$ were tried to see whether one may expect a finite long-range order or a power-decaying correlation function. The results are

$$n^2=-0.0675+13.4559/N-67.6360/N^2, \quad (4.8)$$

$$n^2=N^{-1.1647}(19.7324-108.6654/N). \quad (4.9)$$

The first one (4.8) does not make sense because the limiting value as $N\rightarrow\infty$ is negative. The second fitting function (4.9) is also unreliable since the exponent 1.1647 exceeds 1: If the state is strongly disordered, i.e. paramagnetic, then the leading contribution should be of order $1/N$ as mentioned in §2.3. A larger value 1.1647 apparently signifies inappropriateness of the fitting function (4.9).

Nonetheless 1.1647 is not very far from 1, which suggests that the state may be paramagnetic. We therefore assumed that the leading term is proportional to $1/N$ and fitted the data to the following forms

$$n^2 = 9.609/N - 0.216/N^2 - 344.389/N^3$$

$$(N=9, 21, 27), \quad (4.10)$$

$$n^2 = 1.0743/N + 0.3138N^{1.4949}$$

$$\times \exp(-0.9580\sqrt{N})$$

$$(N=3, 9, 21, 27). \quad (4.11)$$

The first fitting function (4.10) has a very large coefficient in the last term. We do not accept this fitting function because the large coefficient implies even larger coefficients in higher orders leading to instability of expansion. The constants in the second fitting form (4.11) are of acceptable order. For this reason we choose the last form (4.11) as our final result among the four fitting functions from (4.8) to (4.11). The exponential term in eq. (4.11) is obtained by integration of the correlation

$$\langle \sigma_0^x \sigma_r^x \rangle \sim r^{-\eta} \exp(-r/\xi), \quad (4.12)$$

as follows. The lower limit of integration, $r \sim O(1)$, of eq. (4.12) yields a $1/N$ -term while the upper limit, $r \sim O(L) \sim O(\sqrt{N})$, gives the exponential contribution:

$$n^2 \sim a/N + bN^{-(1+\eta)/2} \exp(-c\sqrt{N}/\xi), \quad (4.13)$$

where the constants a , b , c are all of order unity. A comparison of eqs. (4.11) and (4.13) reveals $\xi \sim O(1)$ and $\eta = -4.0$. The latter value of negative η may seem unphysical; as seen in eq. (4.12) the exponent η gives the rate of algebraic decay at a critical point ($1/\xi=0$) and should not be negative. However the present system is paramagnetic ($\xi>0$) even in the ground state. Accordingly the correlation function (4.12) never decays in a power law at any temperature, and therefore the increase of the power factor is always overwhelmed by the exponential decay. We thus find no anomalous increase of correlation even if η is negative.

As a conclusion the spin-spin correlation function is likely to decay exponentially at $T=0$ with correlation length extending a few lattice spacings. This conclusion should be contrasted with Fujiki's¹⁰⁾ preference of an

algebraic decay with $\eta=1.0$ from data of $N=3, 9, 21$.

4.3 Long-range order of chirality

The chirality long-range order (Table VIII) has been analyzed similarly:

$$\langle \chi^2 \rangle = -0.0577 + 8.4632/N - 31.4971/N^2, \quad (4.14)$$

$$\langle \chi^2 \rangle = N^{-1.2500}(15.7732 - 72.6821/N), \quad (4.15)$$

$$\langle \chi^2 \rangle = 5.1755/N + 26.1248/N^2 - 294.340/N^3, \quad (4.16)$$

$$\langle \chi^2 \rangle = 2.6376/N + 0.1239N^{1.7882}$$

$$\times \exp(-1.1487\sqrt{N}). \quad (4.17)$$

The first three equations were derived from $N=9, 21, 27$ data and the last one needed additional data of $N=3$. For the same reasons as in the twisted magnetic order, we would like to choose the last form (4.17) indicating a paramagnetic ground state with $\xi \sim O(1)$ and $\bar{\eta} = -4.6$. Note that FB¹¹⁾ found an algebraic decay from $N=3, 9, 21$ data. Although our fitting function (4.17) also includes data of pure autocorrelation ($N=3$), we believe that the extra data value of $N=27$ makes our analysis more reliable than that of FB.¹¹⁾

We have found that both the twisted magnetic correlation and the chirality correlation decay exponentially in the ground state of the antiferromagnetic spin-1/2 Heisenberg model. The correlation length extends only a few lattice spacings in both cases. Destruction of classical ground-state order (Fig. 5) by quantum effects is most pronounced in the present model among the three systems investigated in this paper. Physical implications are discussed in the next section.

§5. Discussion

By analyzing numerical data for $N \leq 27$ we have found the following properties of the ground states of quantum spin systems on the triangular lattice. The ferromagnetic and antiferromagnetic XY models are likely to be critical at $T=0$; the correlation functions decay in power laws with exponents $\eta(J>0)=0.12$ and $\eta(J<0)=0.34$ for the spin-spin correlation functions and $\bar{\eta}(J<0)=0.15$ for the chirality correlation. The Heisenberg antifer-

romagnet is presumably paramagnetic in the ground state with correlation length of a few lattice spacings. Admittedly it is impossible to exclude finite long-range orders in these systems with greatest confidence since the lattice size is limited to fairly small values. However the lattice size $N=27$ is probably the largest one which can be directly diagonalized on the current computing facilities. (The next size is $N=36$ if one takes only multiples of three.) One has to resort to other methods to confirm or disprove our conclusions. Some of the other approaches are described below, but the present extrapolation technique appears the most systematic one. Before looking at other studies, we discuss some of the consequences of the absence of long-range order assuming validity of our conclusions.

As mentioned in the Introduction the spin wave theory ($1/s$ -expansion) predicts no infrared instability in the ground state of two-dimensional systems. This means that a finite long-range order in the classical case is not destroyed by quantum-mechanical perturbation. The absence of long-range order, therefore, is caused by some non-perturbative mechanism. A possible picture has been proposed by Anderson as a resonating valence bond (RVB) state for the antiferromagnetic Heisenberg model.⁶⁾ Our conclusion of the paramagnetic ground state in this model is not incompatible with the RVB assumption. Even if the RVB state for the antiferromagnetic Heisenberg model is the correct description, we have to look for another origin for the power decay of correlations in the XY model. The fact that both ferromagnetic and antiferromagnetic XY models do not have long-range order leads to the speculation that frustration is not essential in the (unknown) non-perturbative mechanism. If the non-frustration-originated mechanism is operative in the XY models, one is inclined to guess that the same mechanism works in the Heisenberg case. This line of consideration suggests a universal mechanism for all of the present models.

Let us now turn to particular aspects of each model. The ferromagnetic XY model has a critical exponent $\eta=0.12$ at $T=0$. According to Kosterlitz and Thouless¹⁸⁾ a topological

phase transition occurs in this model at a temperature where η reaches $1/4$. In the classical case the $\eta(T)$ is a monotonic function of the temperature increasing from its ground state value 0 to $1/4$ at T_c . Quantum fluctuations reduce the classical order to a level of $\eta=0.12$ at $T=0$, but the system is still able to reach its critical point with $\eta=1/4$ by monotonically increasing η with increasing temperature from $T=0$. Thus a Kosterlitz-Thouless transition is possible to take place in the spin- $1/2$ XY ferromagnet on the triangular lattice. Note, however, that this argument only shows the fulfillment of a necessary condition for a Kosterlitz-Thouless-type transition and never of a sufficient condition. In fact Rogiers *et al.*¹⁹⁾ disputed this point from high-temperature series analysis. Quantum Monte Carlo simulation has been performed,²⁰⁾ the results of which indicate the existence of a finite transition temperature, but no conclusive answer has been given to the type of the transition.

The antiferromagnetic XY model has $\eta=0.34(>1/4)$ already in the ground state. Consequently the system is impossible to have a Kosterlitz-Thouless transition in marked contrast to the classical counterpart.¹⁷⁾ Even the chirality long-range order is destroyed at $T=0$ ($\bar{\eta}=0.15$). A finite temperature transition, if any at all, would be of quite different character from its classical version.¹⁷⁾

The antiferromagnetic Heisenberg model is likely to be paramagnetic at $T=0$. One expects no finite-temperature transition, which is supported by numerical calculations.^{21,22)} Kawamura and Miyashita^{23,24)} have claimed to find a new type of phase transition, a dissociation transition of Z_2 vortices, in the classical case. Although it is impossible to deny this sort of phenomenon in the quantum system, detection of accompanying subtle singularities would be quite difficult.

The ground state properties of the present systems have been investigated by various authors. Comparisons with our results are made in the following although they are never exhaustive. Our values of the ground-state energy are very close to those of FB,⁸⁻¹⁰⁾ as naturally expected from stability of short-range order with respect to the increase of system size. Other methods yield rather scat-

tered values. Some of them are listed in FB's papers,⁸⁻¹⁰⁾ which we avoid to repeat here. (Additional prediction of $E_0/3N|J| = -0.344$ was made by Oguchi *et al.*²⁵⁾ recently for the Heisenberg antiferromagnet.) We mention here only that the second order spin wave expansion^{26,27)} gives close results to ours. This fact is somewhat puzzling because, as has been stressed repeatedly, spin wave theory predicts a finite long-range order in contradiction to our conclusion. Concerning long-range order, FB⁸⁻¹¹⁾ give different conclusions from ours on the twisted order in the antiferromagnetic Heisenberg model (power decay) and on the chirality order in *XY* and Heisenberg antiferromagnets (finite value in the former and a power decay in the latter). Source of difference is solely in the system size. We are thus entitled to claim increased reliability. Nevertheless, as is always true in any numerical study, one should be aware of the possibility that investigation of still larger systems (which is not feasible at present) could upset our conclusions. Numerical study has also been carried out by Oguchi *et al.*⁷⁾ They concluded that the antiferromagnetic *XY* model possesses a finite long-range order whereas the Heisenberg antiferromagnet does not. Their double extrapolation to the infinite size inevitably leads to large uncertainties in quantitative analysis. Qualitatively their data are interpreted as indicating a larger ordering in the *XY* model than in the Heisenberg case. This tendency is consistent with our present findings. The variational approach of Suzuki and Miyashita^{28,29)} has a classical picture behind their quantum mechanical trial function: For instance, in the ferromagnetic case, their zeroth order function has a definite total spin quantum number, the maximum possible value in fact, which is clearly a classical symptom. Thus it is natural that they predicted a finite long-range order, which is incompatible with our conclusion. New approaches, both analytical and numerical, are waited for to further clarify the properties of the two-dimensional quantum spin systems.

Acknowledgment

We thank S. Fujiki and D. D. Betts for pointing out errors in the initial manuscript and useful comments.

References

- 1) P. W. Anderson: Phys. Rev. **86** (1952) 694.
- 2) R. Kubo: Phys. Rev. **87** (1952) 568.
- 3) F. J. Dyson: Phys. Rev. **102** (1956) 1217.
- 4) A. Luther and I. Peschel: Phys. Rev. **B12** (1975) 3908.
- 5) H. Nishimori: Prog. Theor. Phys. **73** (1985) 1577.
- 6) P. W. Anderson: Mater. Res. Bull. **8** (1973) 153.
- 7) T. Oguchi, H. Nishimori and Y. Taguchi: J. Phys. Soc. Jpn. **55** (1986) 323.
- 8) S. Fujiki and D. D. Betts: Can. J. Phys. **64** (1986) 876.
- 9) S. Fujiki and D. D. Betts: Can. J. Phys. **65** (1987) 76.
- 10) S. Fujiki: Can. J. Phys. **65** (1987) 489.
- 11) S. Fujiki and D. D. Betts: Prog. Theor. Phys. Suppl. No. 87 (1986) 268.
- 12) G. Toulouse: Commun. Phys. **2** (1977) 115.
- 13) D. C. Mattis: Phys. Rev. Lett. **42** (1979) 1503.
H. Nishimori: J. Stat. Phys. **26** (1981) 839.
- 14) H. Nishimori and Y. Taguchi: Prog. Theor. Phys. Suppl. No. 87 (1986) 247.
- 15) L. D. Landau and E. M. Lifshitz: *Quantum Mechanics* (Pergamon, London, 1977) 3rd ed., p. 378.
- 16) J. Villain: J. Phys. **C10** (1977) 1717.
- 17) S. Miyashita and H. Shiba: J. Phys. Soc. Jpn. **53** (1984) 114.
- 18) J. M. Kosterlitz and D. J. Thouless: J. Phys. **C6** (1973) 1181.
- 19) J. Rogiers, T. Lookman and D. D. Betts: Can. J. Phys. **56** (1978) 409.
- 20) M. Marcu: *Quantum Monte Carlo Methods in Equilibrium and Nonequilibrium Systems*, ed. M. Suzuki (Springer Verlag, Berlin, 1987) p. 64; T. Onogi, S. Miyashita and M. Suzuki: *ibid.* p. 75.
- 21) M. Takasu, S. Miyashita and M. Suzuki: Prog. Theor. Phys. **75** (1986) 1254.
- 22) M. Imada: J. Phys. Soc. Jpn. **56** (1987) 311.
- 23) H. Kawamura and S. Miyashita: J. Phys. Soc. Jpn. **53** (1984) 9.
- 24) H. Kawamura and S. Miyashita: J. Phys. Soc. Jpn. **53** (1984) 4138.
- 25) T. Oguchi, H. Kitatani and H. Nishimori: J. Phys. Soc. Jpn. **56** (1987) 3858.
- 26) H. Nishimori and S. J. Miyake: Prog. Theor. Phys. **73** (1985) 18.
- 27) S. J. Miyake: Prog. Theor. Phys. **74** (1985) 468.
- 28) M. Suzuki and S. Miyashita: Can. J. Phys. **56** (1978) 902.
- 29) S. Miyashita: J. Phys. Soc. Jpn. **53** (1984) 44.